An equilibrium validation technique based on Bayesian inference

M. J. Hole[1]§, G. von Nessi[1], J. Svensson[2] and the MAST team[3]

[1] Research School of Physics and Engineering, Australian National University, ACT 0200, Australia

[2] Max Planck Institute for Plasma Physics, Teilinstitut Greifswald, Germany.

[3] EURATOM/CCFE Fusion Assoc., Culham Science Centre,Abingdon, Oxon OX14 3DB, UK

Abstract. In recent years, Bayesian probability theory has been used in a number of experiments to fold uncertainties and interdependencies in the diagnostic data and forward models, and together with prior knowledge of the state of the plasma, thus increase accuracy of inferred physics variables. Key developments include the application to current and flux surface tomography, effective charge, the electron energy distribution function, neutron spectrometry, and density. Virtual observations have also been introduced to better constrain inferred quantities in current tomography. In this work we present Bayesian inference results of toroidal and poloidal current and flux surface tomography. While the uncertainty in these profiles, as well as the uncertainty in inferred parameters such as the safety factor profile is small ($<$5%), the inference can change substantially depending on the physics model used. We also present Bayesian inference results for Thomson Scattering and charge exchange recombination spectroscopy. In separate work we have computed radial force balance components on the midplane in the Mega Ampére Spherical Tokamak. Our aim has been to establish a validation framework for different equilibrium physics models. We find that in the overlapping region of the core (normalised poloidal flux less than 0.4) and motional Stark effect (MSE) chords, the plasma is consistent with static Grad-Shafranov force balance to within two standard deviations. In the outboard edge region, where MSE data is also available, the pressure gradient exceeds the Lorentz force. Most likely, this is because the poloidal current is not constrained to zero at the plasma edge. To lowest order, the results suggest computing components of force balance are useful to assess data-consistency, independent to any equilibrium solution. Future work will focus on reducing the uncertainty to validate models with rotation and energetic particle pressure and anisotropy, and establish the viability of inferring these physics terms by adding a suitable force balance constraint.

PACS numbers: 52.55.-s,52.55.Fa,

§ To whom correspondence should be addressed(matthew.hole@anu.edu.au)

1. Introduction

Due principally to neutral beam heating, several tokamak experiments now boast plasma toroidal rotation speeds that approach the thermal Mach speed and have significant stored energy (25% of total stored energy [1]) residing in the energetic particle population produced by charge exchange with thermals. Momentum injection from neutral beams can result in central toroidal rotation frequencies up to 37 kHz [2], and poloidal rotation up to speeds of 80 km s^{-1} [3], and recent studies in MAST suggest that the beam injected anisotropy is as much as $p_\perp/p_\parallel = 1.7$. [4] These additional physics affects can modify the plasma configuration.

A parallel development has been the improvement in the diversity, accuracy and resolution of plasma diagnostics. Often however, interpretation requires a detailed knowledge of the plasma equilibrium. For example, inference of the toroidal current profile J_ϕ from line of sight measurements of the polarization angle requires a knowledge of the poloidal flux ψ across the plasma. A second example, more pertinent to the theme of energetic particle corrections, is that the energetic particle pressure and anisotropy is normally computed by a Monte Carlo orbit simulation, computed assuming a prescribed equilibrium. At present, there are no diagnostics available to measure energetic particle pressure and anisotropy, so the confirmation of their existence is indirect through measuring their impact on equilibrium self-consistency and particle confinement (*e.g.* energetic particle loss detector). The former is often iterative, with the equilibrium progressively corrected to include new physics. [1]

Combined, the improvements in plasma performance, increased diagnostic diversity, additional diagnostic cross-dependency and model inter-dependency suggests the need for an inference framework which formally captures uncertainties in the data $\mathbf{D}$, the plasma parameters $\mathbf{I}$, the forward model for the diagnostic $\mathbf{D}|\mathbf{I}$, and the global equilibrium model. Such a framework should be able to verify different equilibrium descriptions, and offer the possibility to infer otherwise difficult to diagnose properties, such as the energetic particle pressure.

The Bayesian approach to inference in fusion plasmas, developed by multiple authors, [5, 6, 7, 8] involves the specification of an initial prior probability distribution function (pdf), $P(\mathbf{I})$, which is then updated by taking into account information that the measurements provide through the likelihood pdf $P(\mathbf{D}|\mathbf{I})$. The result is the posterior distribution $P(\mathbf{I}|\mathbf{D})$ given by Bayes formula

$$P(\mathbf{I}|\mathbf{D}) = P(\mathbf{D}|\mathbf{I})P(\mathbf{I})/P(\mathbf{D}). \tag{1}$$

The advantage of the Bayesian approach over traditional inversion techniques is two-fold: (i) prior knowledge, including known parameter inter-dependencies is made explicit, and (ii) as the formulation is probabilistic, random errors, systematic uncertainties and instrumental bias are integral part of the analysis rather than an afterthought. We have implemented Bayesian inversion using the MINERVA framework. [9] Within this framework, probabilistic graphical models are used to project the dependence of the posterior distribution function on the prior, the data, and the likelihood. An advantage of this approach is that it visualises the complex interdependency between data and model, and thus expedites model development.

In previous work we have reported on development of MINERVA for toroidal current tomography in MAST, folding together the vacuum toroidal field, pickup coil data, flux loops, and the polarisation angle of emitted light from neutrally excited species during neutral beam injection due to the Motional Stark Effect. [10] One valuable piece of information poloidal flux inference provides is the safety factor or q profile and its associated uncertainty. To date, we have corrected the vacuum toroidal field to account for poloidal currents by using the static Grad-Shafranov equation as an external constraint, folding in measurements of the toroidal current density and pressure gradient modelled outside of MINERVA [10, 11], and inferring the toroidal magnetic flux function. Those works showed that the inclusion of a poloidal current model for MAST yielded a 5% increase in q on axis, and a 5% decrease in q at the edge. The inclusion of a diamagnetic loop in the MINERVA framework, together with a toroidal flux function model, enabled the extraction of poloidal currents within the MINERVA framework [12]. In other work, we have shown how Tikhonoff regularisation combined with diagnostic cross-validation can be combined to form a new technique, "Tikhonoff Cross-Validation", used to remove faulty diagnostics. [13]

In 2010 we have implemented a toroidal flux function, developed Bayesian inference models for electron temperature and pressure from Thomson scattering (TS) data, and developed Bayesian inference models for ion temperature and ion flow profiles parallel to neutral beam lines of sight using charge exchange recombination spectroscopy (CXRS) data. In this work we publish first results on modelling both poloidal and toroidal currents in MAST within a Bayesian inference framework, and present first results on the modelling and Bayesian inference of electron temperature T_e and electron density n_e from TS data, as well as ion temperature T_i and ion flow velocity v_i from charge exchange recombination spectroscopy. In separate working, using analysed temperature and density data, we compute force balance contributions $\mathbf{J} \times \mathbf{B}$, ∇P, and $\rho(\mathbf{v} \cdot \nabla)\mathbf{v}$, and their uncertainty, across the midplane. The purpose of these calculations is to establish a validation technique to distinguish between more sophisticated equilibrium models, which capture flow, anisotropy, and multiple-species.

2. Bayesian current tomography in MAST

Our development of Bayesian inference of the current profile on MAST, detailed in Hole *et al* [10], closely follows the seminal work of Svensson and Werner. [14] In that work, the plasma was represented as a grid of toroidal axis-symmetric current beams, each with rectangular cross-section and each beam carrying a uniform current density. In MAST, we have placed these beams so as to fill-out the entire plasma volume, including regions outside the last closed flux surface up to the vacuum poloidal field coils. The magnetic field generated is then a summation of Biot-Savart's law over current beams.

Here, we build on the results of Hole *et al* [11], who showed current tomography and q profiles computed using MINERVA for discharge #22254. Specifically, we have implemented a poloidal current model via a toroidal flux function $f(\psi) = RB_\phi$. This function satisfies $\nabla \cdot \mathbf{J} = 0$ and $\nabla \cdot \mathbf{B} = 0$, but disallows radial currents that may arise due to the flow of energetic particles. [15] The function $f(\psi)$ is represented by linear interpolation of a set of free parameters f_i distributed uniformly in poloidal flux between the magnetic axis and separatrix.

Figure 1 shows the toroidal current beam and poloidal flux surfaces from MAST discharge #24600 at 280 ms using pickup coils, flux loops, motional Stark effect (MSE) and Rogowski coil data. Discharge #24600 was a deuterium plasma in a double-null configuration, which was heated with 3 MW of neutral beam heating and a plasma current of $I_p = 0.8$ MA. The time of 280 ms analyzed here is the high-resolution TS time closest to the peak β_N. Detailed inspection of Fig. 1(a), which shows the inferred toroidal current beams, reveals that currents were peaked at 0.5 m and 1.1 m on the midplane adjacent to the magnetic axis. A sum over the toroidal currents reveals that 3.6% of the current lies outside the last closed flux surface. Figure 1(b) shows a contour plot of $\psi(R, Z)$, which is calculated from the maximum of the posterior of the distribution of toroidal current beams, and Fig. 1(c) shows a selection of flux surfaces and their uncertainty. In Bayesian inference, the uncertainty in an inferred parameter is computed by sampling different realizations from the (generally not analytically tractable) posterior. Overlaid on all contours are traces of the poloidal field coil cross sections and conducting surface cross sections for the MAST experiment, as well as the last closed flux surface calculated from the plasma beam model and the corresponding EFIT last closed flux surfaces.

Figure 2 shows the MINERVA inferred safety factor or q profile as a function of normalised flux and the toroidal flux function across the midplane, for models with and without a poloidal current. For each model both the expectation and uncertainty are shown, with the latter representing one standard deviation either side of the expectation. In the absence of a poloidal current the q profile is monotonic, and the toroidal flux function constant, taking the vacuum value. The presence of poloidal currents results in a increased core safety factor and a decrease in q in the outer region: indeed, the q profile becomes reverse shear. This increased core safety factor is due to paramagnetic poloidal currents in the core, which strengthen B_ϕ. The zero shear point, at $\psi_n \approx 0.4$, corresponds to the crossing of the poloidal-current-modified toroidal flux with the vacuum toroidal flux function, and in the outer region q is below that of a constant toroidal flux function. Inspection of soft X-ray data shows no evidence of sawtooth activity throughout the discharge, and at 280ms there is no evidence of MHD activity, thereby offering no information to corroborate either model. Our results: (i) demonstrate small uncertainty (*e.g.* $\approx 5\%$ for q) per particular physics model, and (ii) illustrate the model dependence of profile results, and qualify that the quoted uncertainty relates to a particular model, and do not capture the uncertainty due to different models. Despite the limitations, this is the first time q profile uncertainties have been self-consistently computed probabilistically allowing for both toroidal and poloidal currents. We are presently developing a Bayesian framework which employs force balance as a constraint, but provides a statistical confidence measure to differentiate between different models.

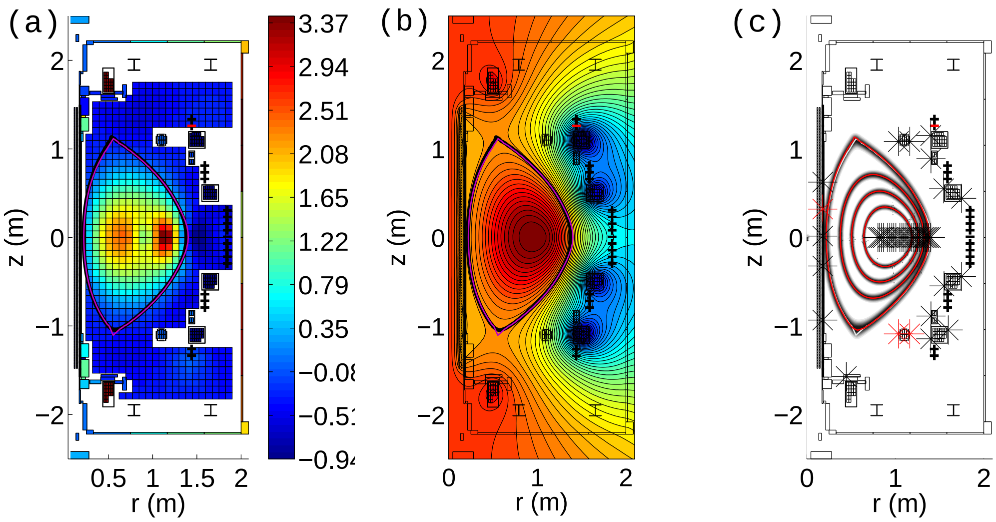

Figure 1. Toroidal current beams and poloidal flux surfaces inferred for MAST discharge #24600 at 280ms using pickup coils, flux loops and MSE. The figure shows the maximum of the posterior distribution function for (a) the toroidal current and (b) the flux surfaces, while figure (c) shows a selection of flux surfaces and their uncertainty. In all figures the solid bars represent pick up coils, in figure (b) the solid black and magenta lines are the EFIT and Bayesian-inferred last closed flux, and in figure (c) the cross-hairs denote the position of the MSE chords and flux loops.

3. Thomson Scattering and Charge Exchange Recombination Spectroscopy

We have implemented Bayesian inference for the Thomson scattering diagnostic and charge exchange recombination spectroscopy. The forward model for TS is based on Scannell [16] and Scannell *et al* [17, 18]. Other analyses of TS using Bayesian probability include Millar *et al* [19], Fischer *et al* [20] and Ford *et al* [21]. We have also implemented Bayesian inference for the Charge Exchange Recombination diagnostic. The forward model is based on the work of Wisse [22].

Figure 3 shows a Bayesian inference for the expectation of electron density n_e and temperature T_e, together with Bayesian inference of the most probable charge-exchange emission intensity, ion temperature and ion flow speed parallel to line of sight at intersection with neutral beam. For the CXRS inference in this discharge, background spectra are treated as nuisance parameters whose construction is based on a linear interpolation between the south west neutral beam lines-of-sight and passive lines-of-sight. These parameterised background spectra are subtracted from the active

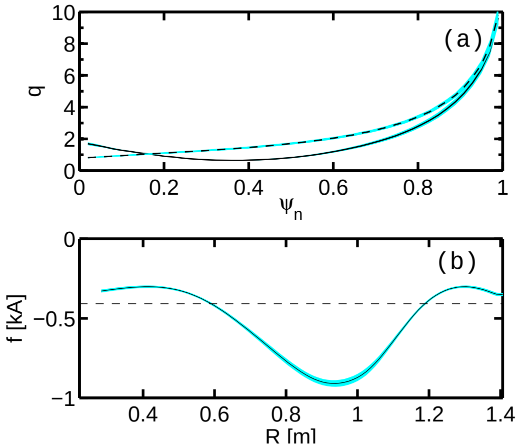

Figure 2. Profiles of (a) safety factor q profile as a function of normalized poloidal flux, and (b) toroidal flux function across the midplane for discharge #24600 at 320ms. The poloidal flux is normalized such that $\psi_n = 0$ is the magnetic axis and $\psi_n = 1$ is the edge. In both figures the dashed line represents the solution without poloidal currents.

spectra during the CXRS forward modelling procedure to yield profiles, which have a direct correspondence to T_i and ion flow profiles parallel to the active line of sight. A sampling analysis of these results, which will yield uncertainty estimates, will be presented elsewhere.

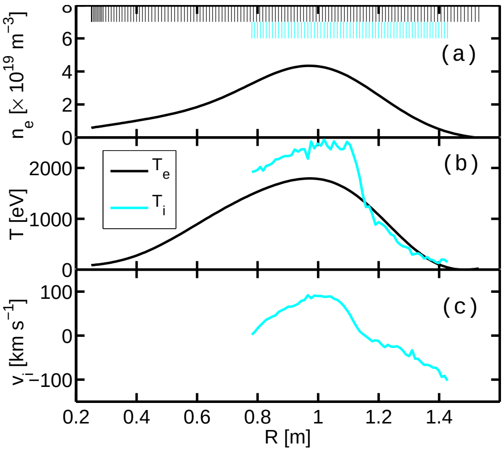

Figure 3. Bayesian inference of electron density and temperature (black) from Thomson scattering, and ion temperature and flow velocity (cyan) from charge exchange recombination spectroscopy: both are for discharge #24600 at 280ms. Figure (a) shows n_e, (b) T_e and T_i and (c) ion velocity. In (a), the vertical lines at the top of the figure denote the radial position of the TS chords (black) and CXRS chords (cyan).

4. Bayesian force balance

In separate calculations we have used the Bayesian framework to compute radial force balance contributions $\mathbf{J} \times \mathbf{B}, \nabla P$, and $\rho(\mathbf{v} \cdot \nabla)\mathbf{v}$ and their uncertainty, across the midplane. In the cylindrical coordinate system R, ϕ, Z, the components are thus

$$\mathbf{J} \times \mathbf{B} \cdot \mathbf{e_R} = J_\phi B_z - B_\phi J_z \tag{2}$$

$$\nabla P \cdot \mathbf{e_R} = \partial P / \partial R \tag{3}$$

$$\rho(\mathbf{v} \cdot \nabla)\mathbf{v} \cdot \mathbf{e_R} = -\rho v_\phi^2 / R \tag{4}$$

with $\mathbf{e_R}$ the $\mathbf{R}$ unit vector, and the field components $B_R = -\frac{1}{R}\frac{\partial \psi}{\partial Z}, B_Z = \frac{1}{R}\frac{\partial \psi}{\partial R}$ and $B_\phi = f(\psi)/R$. For the velocity vector field we have assumed $\partial v_r/\partial r = \partial v_r/\partial \phi = \partial v_r/\partial z = 0$.

In these calculations the same toroidal current-beam model is used as in Sec. 2 and 3, with poloidal currents modelled by fitting for a toroidal flux function $f(\psi) = RB_\phi$. Unlike the analysis of Sec. 3, electron temperature and density, and its uncertainty, is taken from analysed TS data. Also, the toroidal flow velocity, ion temperature and density is taken from analysed charge exchange recombination spectroscopy data. The total pressure is computed by summing the ion and electron partial pressures. Finally, while no equilibrium model has been assumed, some information about flux surface dependency with rotation has been used to better constrain the position of flux surfaces. Specifically, we have assumed that the toroidal angular rotation velocity can be written $v_\phi = \Omega(\psi)R$, with $\Omega(\psi)$, the toroidal angular frequency, a function of poloidal flux. This ignores the contribution of poloidal flow. [23]

Figure 4 shows the calculation of the force balance terms across the midplane for discharge #24600 at 380 ms. MSE data is available in the region $0.7 < R < 1.5$, and so model-data comparison is only meaningful over this range. Within the region $0.6 < R < 1.2$, agreement between the $\mathbf{J} \times \mathbf{B}$ term and ∇p is within two standard deviations. In the core ($0.89 < R < 1.10$), the Lorentz force exceeds the sum of thermal pressure and inertial terms by two standard deviations. Either side of the core, regions of increased uncertainty exist. Combined, these may be consistent with the absence of energetic-particles in this model, which normally produce a pressure profile more localised than the thermal species. A much larger and statistically significant uncertainty exists at the outboard edges. It is likely these arise because the currents are not constrained to zero at the plasma edge.

5. Conclusions

We have developed Bayesian inference for current tomography comprising toroidal current beams and a toroidal flux function, thus modelling poloidal currents. The model is constrained by magnetic pick-up coils, flux loops, MSE data, and the total plasma current. These are first results on the use of Bayesian inference to compute poloidal and toroidal currents within a probabilistic framework. A feature of the Bayesian approach is the generation of pdfs of inferred quantities (such as the safety factor q) from which the

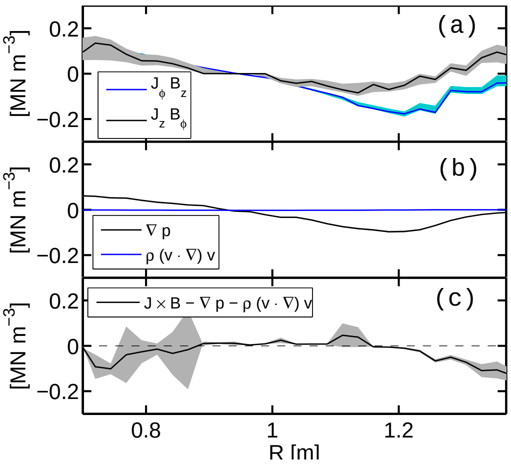

Figure 4. Radial force balance terms and their uncertainty across the midplane chord of MAST #24600 at 320ms. Figure (a) shows elements of $J \times$B, (b) shows ∇P and mass flow term, and (c) shows residual force.

uncertainty can be inferred. Our results (i) demonstrate small uncertainty in inferred parameters (*e.g.* $\approx$ 5% for q) per particular physics model, and (ii) illustrate the model dependence of profile results, and qualify that the quoted uncertainty relates to a particular model, and does not capture the uncertainty due to different models. We have also developed Bayesian inference for Thomson scattering and charge exchange recombination spectroscopy data.

In separate work we have computed radial force balance terms across the midplane. Our purpose has been to develop an equilibrium validation framework to compare and contrast different equilibrium models. We find that in the region where MSE data is available, that although Grad-Shafranov is a reasonable model for the plasma, weak evidence exists for the presence of beam produced energetic ions. To lowest order, our results suggest computing components of force balance are useful to assess data-consistency, independent to any equilibrium solution. We are presently developing a Bayesian framework which employs force balance as a constraint, but provides a statistical confidence measure to differentiate between different models. Future work will focus on reducing the uncertainty to validate models with rotation and energetic particle pressure and anisotropy, and establish the viability of inferring these physics terms by adding a suitable force balance constraint.

Acknowledgments

This work was partly funded by the Australian Government through Australian Research Council grant FT19899 and International Science Linkages Grant CG130047 and the Australian National University. The work by the MAST team was funded by the RCUK Energy Programme under grant EP/I501045 and the European Communities under the contract of Association between EURATOM and CCFE. The views and opinions expressed herein do not necessarily reflect those of the European Commission.

The authors would like to acknowledge Rory Scannell, of CCFE, in providing detailed information on the Thomson Scattering diagnostic in MAST, and Marco Wisse of the University of Basel (Switzerland) for providing detailed information on the charge exchange recombination spectroscopy diagnostic on MAST.

References

[1] M.J. Hole, R.J. Akers, L.C. Appel, R.J. Buttery, C. Brickley, N.J. Conway, M. Gryaznevich, T.C. Hender, O.J. Kwon, M. Valovic, S. Medvedev, A. Patel, S. Saarelma, D. Taylor, H.R. Wilson, and the MAST Team. Ideal MHD stability of the mega-ampere spherical tokamak. *Plasma Phys. Controlled Fusion*, 47:581–613, 2005.

[2] Cottrell GA, Baranov YF, Challis CD, Gormezano C, Ekedahl A, Huysmans GTA, Litaudon X, O'Brien D, Rochard F, Sadler GJ, Schild P, Sips ACC, Soldner FX, Tubbing BJD, Ward DJ, and Zwingmann WP. Evolution of internal transport barriers in JET optimised smear plasmas. *Czech. Jnl. of Phys.*, 48(Suppl. 3):9–24, 1998.

[3] K. Crombé, Y. Andrew, M. Brix, C. Giroud, S. Hacquin, N. C. Hawkes, A. Murari, M. F. F. Nave, J. Ongena, V. Parail, G. Van Oost, I. Voitsekhovitch, and K.-D. Zastrow. Poloidal Rotation Dynamics, Radial Electric Field, and Neoclassical Theory in the Jet Internal-Transport-Barrier Region. *Phys. Rev. Lett.*, 95:155003, 2005.

[4] M. J. Hole, G. von Nessi, M. Fitzgerald, K. G. McClements, and the MAST team. Identifying the impact of rotation, anisotropy and energetic particles in tokamaks. *Plas. Phys. Con. Fus.*, submitted 24/01/2011.

[5] G. A. Cottrell. *Maximum Entropy in Action*, chapter Maximum entropy and plasma physics. Oxford Science, Oxford, 1990.

[6] R Fischer, A Dinklage, and E Pasch. Bayesian modelling of fusion diagnostics. *Plas. Phys. Cont. Fus.*, 45:1095–1111, 2003.

[7] J Svensson, A Dinklage, J Geiger, A Werner, and R Fischer. Integrating diagnostic data analysis for W7-AS using Bayesian graphical models. *Rev. Sci. Instrum.*, 75(10):4219–4221, Jan 2004.

[8] Oliver Ford. *Tokamak Plasma Analysis through Bayesian Diagnostic Modelling*. PhD thesis, Imperial College, London, November 2010.

[9] J Svensson and A Werner. Large scale bayesian data analysis for nuclear fusion experiments. *IEEE International Symposium on Intelligent Signal Processing*, pages 1–6, Jan 2007.

[10] M. J. Hole, G. von Nessi, J. Bertram, J. Svensson, L. C. Appel, B. D. Blackwell, R. L. Dewar, and J. Howard. Model Data Fusion: developing Bayesian inversionto constrain equilibrium and mode structure. *Journal of Plasma and Fusion Research*, 9, 2010.

[11] M. J. Hole, G. von Nessi, D. Pretty, J. Howard, B. Blackwell, J. Svensson, and L. C. Appel. The use of Bayesian inversion to resolve plasma equilibrium. *Rev. Sci. Instrum.*, 2010.

[12] L. C. Appel, M. J. Hole, J. Svensson, G. von Nessi, and the MAST team. Bayesian Inference as applied to Magnetic Equilibrium on MAST. In *EPS 37th Conference on Plasma Physics and Controlled Fusion*, Dublin, 21-25 June, 2010.

[13] G. T. von Nessi, M. J. Hole, J. Svensson, and L. Appel. Evidence Cross-Validation and Bayesian Inference of MAST Plasma Equilibria. *Phys. Plas.*, 2011. submitted 29/03/2011.

[14] J. Svensson and A. Werner. Current Tomography for Axisymmetric Plasmas. *Plas. Phys. Con. Fus.*, 50(085002), 2008.

[15] K. G. McClements and A. Thyagaraja. Collective electric field effects on the confinement of fast ions in tokamaks. *Phys. Plas.*, 13:042503, 2006.

[16] Rory Scannell. Investigation of H-mode edge profile behaviour on MAST using Thomson scattering. *Ph.D. Thesis*, 2007.

[17] R. Scannell, M. J. Walsh, P. G. Carolan, A. C. Darke, M. R. Dunstan, R. B. Huxford, G. McArdle, D. Morgan, G. Naylor, T. O'Gorman, S. Shibaev, N. Barratt, K. J. Gibson, G. J. Tallents, and

H. R. Wilson. Design of a new NdYAG Thomson scattering system for MAST. *Rev. Sci. Instrum.*, 79:10E730, 2008.

[18] R. Scannell, M. J. Walsh, M. R. Dunstan, J. Figueiredo, G. Naylor, T. O'Gorman, S. Shibaev, K. J. Gibson, and H. Wilson. A 130 point Nd:YAG Thomson scattering diagnostic on MAST. *Rev. Sci. Instrum.*, 81:10D520, 2010.

[19] A. P. Millar, D. C. McDonald, and D. A. Diver. Genetic algorithms in plasma diagnostic analysis. *Plas. Phys. Cont. Fus.*, 42:337–346, 2000.

[20] R Fischer, C Wendland, A Dinklage, S Gori, V Dose, and the W7-AS team. Thomson scattering analysis with the Bayesian probability theory. *Plas. Phys. Con. Fus.*, pages 1501–1519, 2002.

[21] O. P. Ford, J. Svensson, M. Beurskens, A. Boboc, J. Flanagan, M. Kempenaars, D. C. McDonald, and A. Meakinsand JET EFDA contributors. Bayesian Combined Analysis of JET LIDAR, Edge LIDAR and Interferometry Diagnostics. In *36th EPS Conference on Plasma Physics, Europhysics Conference Abstracts*, number 33E, pages P–2.150, Sofia, Bulgaria, June 29 - July 3.

[22] M. Wisse. *Charge-Exchange Spectroscopy in the MAST Tokamak.* PhD thesis, University College Cork, Ireland, 2007.

[23] M. J. Hole and K. G. McClements. The impact of energetic particles and rotation on tokamak plasmas. *J. Phys. Conf. Ser.*, 260(012013), 2010.